International Journal of Mass Spectrometry 283 (2009) 140–148

Contents lists available at ScienceDirect

International Journal of Mass Spectrometry

journal homepage: www.elsevier.com/locate/ijms

Gas-phase metalloprotein complexes interrogated by ion mobility-mass spectrometry

Peter A. Faull, Karoliina E. Korkeila, Jason M. Kalapothakis, Andrew Gray, Bryan J. McCullough [1], Perdita E. Barran *

School of Chemistry, University of Edinburgh, West Mains Road, Edinburgh, EH9 3JJ, United Kingdom

ARTICLE INFO

Article history:
Received 9 December 2008
Received in revised form 24 February 2009
Accepted 25 February 2009
Available online 13 March 2009

Keywords:
Ion mobility
Metalloproteins
Protein unfolding

ABSTRACT

Gas-phase biomolecular structure may be explored through a number of analytical techniques. Ion mobility-mass spectrometry (IM-MS) continues to prove itself as a sensitive and reliable bioanalytical tool for gas-phase structure determination due to intense study and development over the past 15 years. A vast amount of research interest, especially in protein and peptide conformational studies has generated a wealth of structural information for biological systems from small peptides to megadalton-sized biomolecules. In this work, linear low field IM-MS has been used to study gas-phase conformations and determine rotationally averaged collision cross-sections of three metalloproteins—cytochrome *c*, haemoglobin and calmodulin. Measurements have been performed on the MoQToF, a modified QToF 1 instrument (Micromass UK Ltd., Manchester, UK) modified in house. Gas-phase conformations and cross-sections of multimeric cytochrome *c* ions of the form $[xM + nH^+]^{n+}$ for $x = 1–3$ (monomer to trimer) have been successfully characterised and measured. We believe these to be the first reported collision cross-sections of higher order multimeric cytochrome *c*. Haemoglobin is investigated to obtain structural information on the associative mechanism of tetramer formation. Haemoglobin molecules, comprising apo- and holo-monomer chains, dimer and tetramer are transferred to the gas phase under a range of solution conditions. Structural information on the proposed critical intermediate, semi-haemoglobin, is reported. Cross-sections of the calcium binding protein calmodulin have been obtained under a range of calcium-bound conditions. Metalloprotein collision cross-sections from ion mobility measurements are compared with computationally derived values from published NMR and X-ray crystallography structural data. Finally we consider the change in the density of the experimentally measured rotationally averaged collision cross-section for compact geometries of the electrosprayed proteins.

1. Introduction

Interrogating biological molecules in the gas-phase using ion mobility-mass spectrometry (IM-MS) techniques yield information not available using mass spectrometry alone, opening a new avenue to structural biology [1–3] in particular when coupled with the use of nano-electrospray ionisation (nano-ESI) to probe near-native environments from solutions of biomolecules for analysis by mass spectrometry [4–6]. Still, to date, more molecules have been investigated using mass spectrometry alone over a size range spanning three orders of magnitude, from the hydration of small peptides [7] to large macromolecular protein assemblies [8,9]. Upon transfer to the gas-phase, charged analyte ions are guided through source optics to the first reduced pressure chamber in a mass spectrometer. In many instruments, these initial optics are based on multipoles within a pressure range of 5×10^{-1} to 1×10^{-3} mbar backed by a rotary pump. Recent studies systematically adjusting source hexapole pressure conditions [10–12] provide useful methodology for analysing biomolecules composed of multiple constituent subunits or macromolecular assemblies [13]. Essentially the change in pressure from atmosphere to high vacuum must be achieved slowly to maintain noncovalent interactions and successfully transfer multicomponent structures into the mass spectrometer for subsequent analysis.

Ion mobility spectrometry has been evolving since the early 1970s [14] and adds dimensionality to separating chemical compound mixtures [15], isomers [16] and more recently, to protein or peptide conformations. Commercial mobility instrumentation has recently become available including field asymmetric waveform ion mobility spectrometry (FAIMS) [17,18] and an IM-MS instrument produced by Waters (the Synapt HDMS) which uses travelling wave (T-wave) ion-guides to trap, transmit and focus ions

* Corresponding author. Tel.: +44 131 650 7533.
E-mail address: perdita.barran@ed.ac.uk (P.E. Barran).
[1] Present address: Manchester Interdisciplinary Biocentre, 131 Princess Street, Manchester, M1 7DN, UK.

1387-3806/$ – see front matter © 2009 Elsevier B.V. All rights reserved.
doi:10.1016/j.ijms.2009.02.024

[19,20]. Both instruments have been successfully employed to interrogate complex biomolecules [21,22] possessing multiple gas phase conformers [23]. Despite the certain benefits of commercial instrumentation, the majority of IM-MS work on biomolecules has been performed on home built instrumentation [23–27]. A typical linear low field IMS or IM-MS device will record the time it takes for a given ion to pass through a cell containing a buffer gas at a known pressure and temperature, under the influence of a weak electric field (5–50 V cm^{-1}). As the length of the cell will be known, this drift time can be used to determine the drift velocity for the given ion, with mass analysis occurring before or after this mobility separation. The mobility of an ion (K) is defined as the ratio between the drift velocity and the applied electric field. The rotationally averaged collision cross-section (Ω) of metalloprotein molecules and complexes are directly measured due to the relationship between drift velocity, mobility (K) and Ω [28] (Eq. (1)).

$$K_0 = \frac{3ze}{16N}\left(\frac{2\pi}{\mu k_B T}\right)^{1/2}\frac{1}{\Omega} \quad (1)$$

where K_0 is the reduced mobility (the measured mobility corrected to 273.15 K and 760 Torr), z is the ion charge state, e is the elementary charge, N is the gas number density, μ is the reduced mass of the ion-neutral pair, k_B is the Boltzmann constant and T is the gas temperature.

This study employs IM-MS to examine three metalloproteins. Metalloproteins incorporate a vast number of biological molecules requiring a metal ion cofactor for correct physiological function. Processes such as oxygen transport (haemoglobin), electron transport (cytochrome *c*) and enzyme regulation (calmodulin) are all governed by proteins containing group I, group II or transition metal ions within their structure. Cytochrome *c* may well be considered the most studied biomolecule by mass spectrometry [29] due to its ease of ionisation and availability, as well as the diverse range of conformations it adopts at intermediate charge states ($z \geq 7$). IM-MS and FT-ICR-MS studies have revealed that cytochrome *c* molecules sample a large number of gas-phase conformations when trapped for prolonged time periods in an ion trap mass spectrometer revealing the conformational heterogeneity possible [30,31]. As it contains a covalently bound haem group, cytochrome *c* has been interrogated under a range of dissociation conditions to assess its gas-phase stability in comparison to molecules such as myoglobin or haemoglobin that contain noncovalently bound haem groups [32]. Many gas-phase investigations on haemoglobin have been reported over the past decade with intense focus on interactions between the subunits and between the haem-globin monomer [33–35]. Measuring gas-phase stability using dissociative techniques (e.g., collision induced dissociation) provides evidence for the retention of noncovalent interactions into the gas-phase. Interest in the component globin monomeric chains (α and β), the homodimeric (αβ) species and the biologically active heterotetramer $(\alpha\beta)_2$ has provided information on the assembly and disassembly pathways [36,37]. Asymmetric behaviour of the globin monomer chains in haemoglobin was investigated [38] and provided an insight into the mechanism of tetramer assembly. The α-chain monomer was tightly folded in the holo state (haem bound) and acted as a template for the partially unstructured apo β-chain to organise into a more ordered conformation, allowing for efficient haem acquisition and formation of the haem-containing heterodimer. These observations were surprising given the high sequence homology (~43%) between the α and β chains and served to highlight the importance of intrinsic protein disorder in a field where protein order is frequently the primary focus. Denaturing the haemoglobin complex through addition of acid has recently provided insight into the reason why the α-monomer is observed with a much higher intensity than that of the β-monomer [39]; the α-monomer unfolds to a greater extent and attains a higher ionisation efficiency, thus suppressing the signal of the β-monomer. ESI-MS studies of the mutated haemoglobin H [40], a homotetrameric complex composed of β-globin monomers that is formed *in vivo* as a consequence of β-globin over expression in α-thalassemic disorders, provided conformational evidence of the importance of a well structured α-globin monomer in the heterotetramer assembly process.

Calmodulin (CaM) is a calcium binding protein instigated in function regulation of a wide and diverse range of target enzymes [41,42] and structural proteins. Upon binding calcium into one of four distinct EF binding loops [43], calmodulin undergoes a significant conformational change to form a "dumb-bell"-shaped molecule and exposing a central alpha-helix central linker. It has been proposed [44] that this provides holo-calmodulin with greater interaction ability to target molecules and allows the N- and C-terminals with greater flexibility to roam over the target molecule surface for an optimal complex conformation. In its apo form, CaM has a molecular weight of ~16.7 kDa and is highly conserved between eukaryotic species.

Here, IM-MS data provides cross-sections of three metalloproteins under different solution conditions allowing us to interrogate aggregation, unfolding and the effect of calcium ion incorporation on gas-phase conformation.

2. Experimental

2.1. Materials

Lyophilised human haemoglobin (Sigma–Aldrich, St. Louis, MO, USA) was dissolved in 50 mM ammonium acetate and passed through a PD-10 column (GE Healthcare Bio-Sciences AB, Uppsala, Sweden) to remove any salts prior to analysis. The concentration was measured using a UV/vis spectrometer (Cecil 1000 Series, Progen Scientific Ltd., Nuneaton, UK) at $\lambda = 274$ nm and $\varepsilon_{oxy} = 138{,}048\ M^{-1}\ cm^{-1}$ and established to be 120 μM. Aliquots of stock solution were diluted as appropriate with 50 mM ammonium acetate at pH 6.75. 2% by volume formic acid (GPR Rectapur, VWR International, Fontenay sous Bois, France) was used to acidify sample solutions and induce protein unfolding. 2% by volume formic acid and 50% by volume methanol (Analar Normapur, VWR Interational, Fontenay sous Bois, France) were added to buffered samples to induce further denaturation. Any additional solvents or buffers used were analytical grade or better. Lyophilised equine heart cytochrome *c* was purchased from Sigma–Aldrich (St. Louis, MO, USA) and used without further purification. It was dissolved in distilled water to a concentration of 200 μM at pH 5.65 to induce multimer (homodimer) formation and diluted to the required concentration. Lyophilised bovine brain calmodulin was purchased from Calbiochem (Merck Chemicals, Nottingham, UK). Calcium-free (apo) calmodulin was prepared by addition of 0.4 M EGTA (Sigma–Aldrich, St. Louis, MO, USA) to dissolved protein followed by extensive dialysis against 10 mM ammonium acetate at 4 °C using Slide-A-Lyzer Dialysis Cassettes with a 3500 molecular weight cut off (Pierce Protein Research Products, Thermo Scientific, Rockford, IL, USA). Dialysed protein was then passed through a PD-10 column (GE Healthcare Bio-Sciences AB, Uppsala, Sweden) to remove any salts prior to analysis. Calcium acetate was purchased from Sigma–Aldrich (St. Louis, MO, USA) and an aqueous stock solution of 100 mM was stored at 4 °C until required.

For IM-MS experiments, 5 mM calcium acetate was added to 150 μM apo calmodulin and left to incubate overnight. This solution was diluted threefold (50 μM) in a 50/50 by volume solution of 10 mM ammonium acetate and methanol. 2% formic acid was added prior to analysis.

2.2. Mass spectrometry

All mass spectra were acquired on a modified QToF 1 (Waters, Manchester, UK) [27] quadrupole time-of-flight mass spectrometer containing a 5.1 cm copper drift cell for mobility measurements. Data was analysed using modified MassLynx version 4 software. Ions were produced by positive nano-electrospray ionisation (Z-spray source) within a spray voltage range of 1.2–1.7 kV and a source temperature of 80 °C. Sample and extractor cone voltages were maintained as low as possible so as to avoid in-source dissociation and to maintain stable signal. Nanospray tips were prepared in-house from borosilicate glass capillaries (Kwik-Fil, World Precision Instruments Inc., Sarasota, FL, USA) using a Flaming/Brown Micropipette puller (Model P-97, Sutter Instrument Co., Novato, USA). Capillary tips were optimised for desolvation of multimers and to minimise tips becoming blocked. Tips were filled with 10–15 μL of sample using gel loader tips (Eppendorf, Hamburg, Germany).

2.3. Mobility measurements

MoQTOF operation and measurement acquisition method have been described in detail elsewhere [27]. Briefly, ion mobility experiments were performed at ~3.5 Torr helium pressure and ~300 K cell temperature. The drift voltage across the cell was varied to obtain ion mobility data by decreasing the cell body potential from 70 to 10 V. All mobility data was obtained from plots of arrival time versus drift voltage over this range. Measurements were taken at 7 or more distinct voltages. Nano-electrospray ionisation produces a constant beam of ions which must be trapped to allow discrete ion packets to be pulsed into the drift cell. This is achieved by raising the DC voltage on the top hat lens element directly before the entrance elements to the cell, trapping the ions in the pre-cell hexapole. The trapping DC is then lowered for 40 μs through use of a pulse generator (Stanford Research Systems, Sunnyvale, CA, USA) allowing a pulse of ions into the drift cell. Ions are focused into the drift cell using a three element Einzel lens, separated by mobility within the cell and then accelerated through the quadrupole and ToF mass analysers to a MCP detector. A minimum of 2000 scans were collected for each drift voltage. Data was processed using Microsoft Excel and Origin 7.5 (Origin Lab) to determine collision cross-sections from arrival times over a range of drift voltages.

3. Results and discussion

3.1. Mass spectrometry studies of haemoglobin

3.1.1. Native-like conditions

Blood pH is strictly regulated over a narrow range so as to accommodate the large number of biological and chemical components it contains. Increasing haemoglobin pH to 8.5 has been shown [45] to promote and favour haemoglobin tetramer formation. Decreasing pH to 5.9 promotes dissociation to heterodimer and monomer species. 30 μM haemoglobin in 10 mM ammonium acetate (pH 6.75) was initially investigated here to study both tetrameric and dimeric species [45]. These conditions minimise adduct formation. Although below physiological pH, the buffered solution conditions are herein referred to as "native-like" due to the relative abundance of multimeric species to monomer species.

Fig. 1 shows a mass spectrum of haemoglobin taken from 500 to 3900 *m*/*z*. Dominant peaks can be assigned with relative ease reflecting the amenability of ESI-MS to heterogeneous mixtures. The most intense peaks correspond to α_{holo} with a narrow charge state distribution and a low charge density. This is expected for a holo species that has sufficient preservation of the native fold to retain the haem moiety. As proposed by de la Mora [46], the

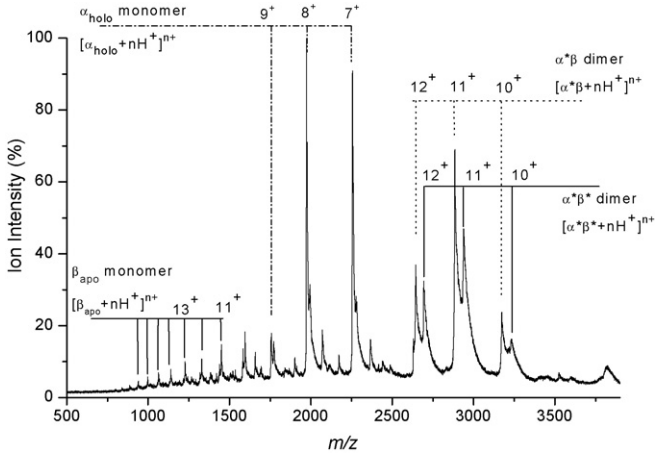

Fig. 1. 30 μM haemoglobin in 10 mM ammonium acetate (pH 6.75) from 500 to 3900 *m*/*z* showing a number of gas-phase multimer species. For clarity, a species present in a multimer that contains a haem bound to it is denoted with an asterisk. In the text if the species is monomeric, a subscript "holo" or "apo" denotes haem bound or no haem bound respectively.

maximum number of charges on a folded protein may be simply estimated as:

$$Z_R = 0.0778\sqrt{M_R} \quad (2)$$

where M_R represents the molecular mass of the protein. From this equation it can be calculated that α_{holo} can sustain approximately ten positive charges which is in good agreement with the highest experimentally observed charge state ($[\alpha_{holo}+9H^+]^{9+}$), providing evidence for the native α_{holo} fold being preserved into the gas-phase. There is no evidence for α_{apo} under these conditions implying α_{holo} is a well organised structure that does not undergo haem-loss or sufficient structural rearrangement in the gas-phase so as to lose the noncovalent interactions necessary for the haem group to be maintained.

A number of peaks at lower *m*/*z* can be attributed to β_{apo} chains. A wide charge state distribution with higher charge densities than that of the α_{holo} chain indicates the β-globin has partially unfolded and lost the haem group. Dissociation of the tetramer to monomer species has destabilised the β-globin structure to a greater extent to that of the α-globin. The absence of β_{holo} peaks implies that it too is less stable than the α_{holo} chain and the wider range of charge states provides evidence for structural heterogeneity. These observations are consistent with previous native haemoglobin studies [38] under these conditions and highlight the greater binding strength of haem to the α-globin chain.

The mass spectrum region above 2500 *m*/*z* shows evidence for dimeric and tetrameric species, indicating conditions were sufficient to preserve some noncovalent interactions and quaternary structure into the gas-phase. Two dimeric species are present: (i) the holoheterodimer $\alpha^*\beta^*$ (M_R 32,255.6 Da) with both globin monomers retaining haem moieties, and (ii) a semi-haemoglobin species with a single haem group bound $(\alpha\beta)^*$ (M_R 31,608.6 Da) [45]. Both dimeric (D) species display narrow charge state distributions centred at $[M+11H^+]^{11+}$ ($M = D_{\alpha^*\beta^*}$ and $D_{(\alpha\beta)^*}$) indicating compact tertiary structure [47]. Unfolding of these species may produce the monomeric globin chains observed at lower *m*/*z*. The semi-haemoglobin species can be assigned as $\alpha^*\beta$ as dissociation of this dimer to α^* and β is evidenced in the mass spectrum (and further clarified by the absence of α and β^* peaks). Tetramer (Q) is observed in the mass spectrum at $[Q+17H^+]^{17+}$ and $[Q+16H^+]^{16+}$ at 3793 and 4030 *m*/*z* respectively. The narrow charge state distribution reflects the compact structure and relative structural homogeneity of the tetramer [38,47]. The highest observed charge

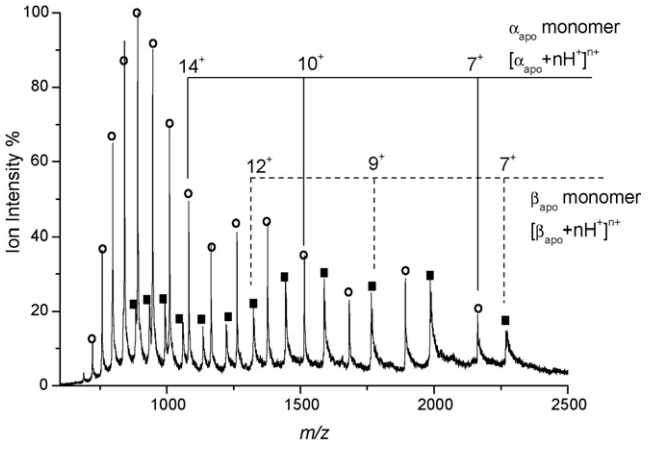

Fig. 2. Mass spectrum upon addition of 2% formic acid to buffered 30 μM haemoglobin samples covering the range 600–2500 *m*/*z*. At this low pH, only haem-deficient globin monomer chains are present. α haemoglobin chains are denoted with the symbol ○ and β chains with the symbol ■.

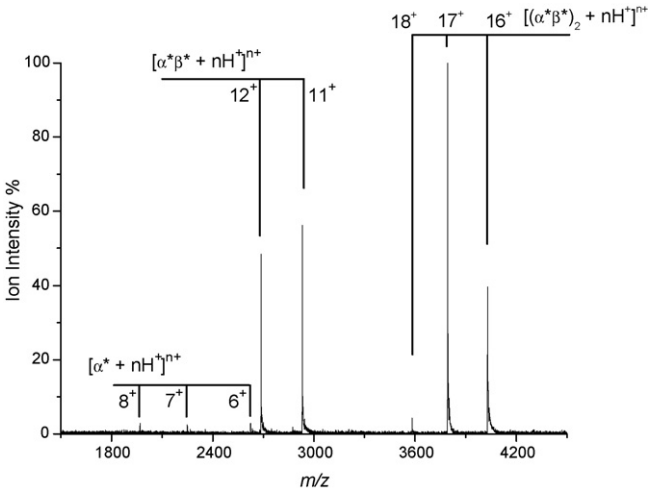

Fig. 3. Mass spectrum of haemoglobin in buffered ammonium acetate at pH 9.5 from 1500 to 4500 *m*/*z*. All observed peaks are annotated. The elevated pH stabilises tetramer signal with the $[Q+17H^+]^{17+}$ tetramer dominating the spectrum. Holoheterodimer and α^* are also present.

state (17^+) is in good agreement with the calculated maximum charge for a compact conformer ($Z_R \sim 20$).

When monomers associate to form higher order structures, basic ionisable sites may become buried within the core of the new complex or at the dimer interface. This may explain why the average dimer charge density per subunit is less than that for the individual monomers since there are fewer sites available to protonation. This would be indicative of a well folded structure and further probing using techniques such as hydrogen/deuterium exchange [48,49] would provide structural information on the solvent accessibility of amino acid residues. The charge density further decreases for the tetramer as the interface size increases [47] as one would expect for a higher order structure requiring a large number of noncovalent interactions.

3.1.2. Denaturing conditions with 2% acid

Addition of 2% formic acid to buffered 30 μM haemoglobin samples reduced the pH to 4.5. Fig. 2 provides a mass spectrum over the range 600–2500 *m*/*z* of this sample, showing a wide charge state distribution and high charge states characteristic of a denatured and unfolded protein [50,51]. Evidence for protein unfolding is further reinforced as detected peaks can be assigned to haem-deficient α_{apo} and β_{apo} globin chains. Both monomer species exhibit a significant degree of unfolding and disordered structure. Haemoglobin has unfolded to the extent that the interactions required to maintain the haem within its discrete binding pocket have been lost. Unbound haem is not soluble under aqueous conditions [32] and so is not detected in the mass spectrum (no peak present at 616 *m*/*z*).

A trimodal charge state distribution provides evidence for three possible α_{apo} conformers in solution equilibrium [52] observed *in vacuo* with (i) unfolded at $[\alpha_{apo} + 17H^+]^{17+}$, (ii) partially unfolded at $[\alpha_{apo} + 12H^+]^{12+}$ and (iii) semi-folded at $[\alpha_{apo} + 8H^+]^{8+}$. The unfolded conformers dominate the distribution. A similar distribution is observed for the β_{apo} monomer with (i) unfolded at $[\beta_{apo} + 16H^+]^{16+}$, (ii) partially unfolded at $[\beta_{apo} + 10H^+]^{10+}$ and (iii) semi-folded at $[\beta_{apo} + 8H^+]^{8+}$. The presence of folded monomers at low charge states but the absence of dimeric species (mass spectrum not shown) confirms that inter-subunit forces are weaker than the intramolecular forces within the globin chains.

3.2. Denaturing conditions with acid and methanol

Upon addition of 50% by volume methanol to the acidified sample, the protein is denatured to a further degree. This results in a decrease in the intensity of low charge states of both the α_{apo} and β_{apo} and a shift to a bimodal high charge state distribution, implying extensive protein unfolding and a small population of potentially semi-folded conformers (data not shown). The presence of two discrete distributions indicates a cooperative "all-or-none" transition from one conformer to the other [50]. The increased organic solvent content promotes observation of the singly charged haem group at 616 *m*/*z*. Once again, no multimeric species were observed under these conditions as one would expect of a highly denatured environment.

3.2.1. Elevated pH for tetramer formation

Increasing the ammonium acetate buffer pH, using sodium hydroxide, to pH 9.5 was shown to elevate the intensity of signal due to tetrameric haemoglobin, consistent with previous work [45]. Three tetramer (Q) signals were clearly apparent $[Q+nH^+]^{z+}$ for $z = 16$, 17 and 18 with *m*/*z* values of 4030.0, 3793.0 and 3582.3 (Fig. 3). This mass spectrum also shows two holoheterodimers ($\alpha^*\beta^*$) with charge states 11^+ and 12^+, along with very weak signals for three α^* monomer species with 6^+ to 8^+ charge states.

3.3. Ion mobility-mass spectrometry studies of haemoglobin

3.3.1. Native-like conditions

A single arrival time peak was observed for all species under native-like conditions from IM-MS experimental data indicating compact structures—not necessarily indicative of a singular gas-phase conformation but perhaps a number of conformations with similar mobilities and cross-sections.

Four α_{holo} monomers were distinguished under these experimental conditions for $[\alpha_{holo}+nH^+]^{z+}$ $z = 6$–9. The collision cross-section increases with increasing charge state (Table 1) with a near linear increase from $z = 7$ to 9 which is attributable to Coulombic repulsion. There is a larger change in cross-section from $z = 6$ to 7 indicating a protein unfolding event.

Ten β_{apo} globin monomers were distinguished: $[\beta_{apo}+nH^+]^{z+}$ for $z = 8$–17. The collision cross-sections are reported in Table 1. Between $z = 8$ and 11, there is a near linear increase in collision cross-section resulting in a total increase of 410 Å^2, a significant increase in the size of the protein. This accommodates the acquired positive charges. In the region $z = 11$–14 the cross-section changes by less than 75 Å^2 which indicates the positive charge is being accepted at sites that are more remote and a large conformational change is not

Table 1
Collision cross-sections (Å^2) of α and β monomer chains under native (10 mM ammonium acetate buffer) and denatured (10 mM ammonium acetate + 2% formic acid) conditions.

Charge	Holo-α (native)	Apo-α (denatured)	Apo-β (native)	Apo-β (denatured)
6	1115	–	–	–
7	1420	1381	–	1421
8	1525	1515	1461	1532
9	1608	1625	1626	1679
10	–	1700	1733	1864
11	–	1863	1871	1941
12	–	2041	1886	2068
13	–	2252	1899	2156
14	–	2441	1945	2267
15	–	2590	2080	2398
16	–	2614	2541	2595
17	–	2772	2622	2679
18	–	3200	–	3057
19	–	3227	–	3147
20	–	3430	–	–
21	–	3465	–	–
22	–	3498	–	–

necessary to reduce the repulsive force. As charge increases further (z = 15 and 16) a dramatic size increase of 596 Å^2 is observed. This large increase could be attributed to the loss of a secondary fold in a significant portion of the monomeric protein.

These large cross-section increases support the suggestion that the β-globin monomer has an intrinsically unstructured nature. Small regions of the protein are potentially structured but addition of charge causes large structural changes—indicating few conserved interactions within the molecule. Under physiological conditions, β_{apo} monomers use α_{holo} monomers as templates to order themselves into a structure capable of binding a haem group subsequently forming the α*β* holoheterodimer of which were distinguished: $[\alpha^*\beta^*+nH^+]^{z+}$ for z = 10–12. Collision cross-sections for all three dimers (Table 1) imply minimal protein unfolding with increasing protonation. Also of interest is the fact that the dimer cross-section is less than twice that of the monomers that could produce it, indicative of re-ordering by the monomer subunits to adopt a more compact dimer.

The α*β semi-haemoglobin dimer has been proposed as a crucial intermediate in the assembly pathway for the biologically active tetramer [38,40,53]. Three semi-haemoglobin dimers were observed here: $[\alpha^*\beta+nH^+]^{z+}$ for z = 10–12 (Table 1). The collision cross-sections of the semi-haemoglobin and holo heterodimers are within 5% of one another of the same z value, indicating that for these gas-phase conformations, loss of a haem group through structural rearrangement and loss of noncovalent bonding has altered the collision cross-section only to a small extent.

The $(\alpha^*\beta^*)_2$ tetramer was observed with at 3394 and 3520 m/z relating to $[(\alpha^*\beta^*)_2+16H^+]^{16+}$ and $[(\alpha^*\beta^*)_2+17H^+]^{17+}$ respectively. A narrow charge state distribution indicates a well folded tetramer in the gas-phase showing that preservation of noncovalent interactions is sustained. There is a small (∼4%) increase in collision cross-section between z = 16 and 17, suggesting charge sequestering at a site that does not induce a large conformational change to overcome unfavourable interactions. Higher charge states were not observed as expected since higher charge would potentially destabilise the complex and cause dissociation, lowering the tetramer signal and increasing lower ordered species signals.

3.3.2. Denaturing conditions with acid

Upon protein denaturation, monomer globin chains of α_{apo} and β_{apo} were observed in the mass spectrum, and more species with higher numbers of protons are observable, as expected from a lower pH solution. Their collision cross-sections are reported in Table 1.

Table 2
Collision cross-sections (Å^2) of α*β dimer, α*β* dimer and $(\alpha^*\beta^*)_2$ tetramer haemoglobin species. Dimer species data was collected under native conditions (10 mM ammonium acetate). For all five tetramer species, data was collected upon elevating the buffer pH to 9.5.

Charge	α*β dimer	α*β* dimer	$(\alpha^*\beta^*)_2$ tetramer
10	2225	2174	–
11	2249	2355	–
12	2469	2484	–
13	–	–	3051
14	–	–	3215
15	–	–	3408
16	–	–	3460
17	–	–	3649

At low charge states, α_{apo} cross-sections are smaller than β_{apo} indicating a more compact and folded structure due to a lack of solvent-accessible protonation sites causing protein unfolding. Collision cross-section increases near linearly with charge state due to unfolding to overcome Coulomb repulsion. However at higher charge states it is apparent that either a more complicated unfolding mechanism is occurring or that the unfolding is not attributable to Coulomb repulsion. Possible exposure of a region rich in ionisable sites sees a greater increase in cross-section with subsequent protons. At z = 13, the α_{apo} monomer collision cross-section is larger than the β_{apo} indicating the (-globin monomer has lost its structural integrity and begun to unfold to a greater degree.

3.3.3. Denaturing conditions with acid and methanol

Collision cross-sections for both globin chains increase upon methanol addition as it acts as a denaturant at high concentrations, increasing protein unfolding and exposing the hydrophobic core (and potentially more basic sites). Methanol also acts to stabilise secondary helical structure at lower concentrations. At low charge states, collision cross-sections increase in small increments as solvent accessible sites are protonated (Table 1). At higher charge states, the protein will unfold due to Coulombic effects. As this occurs methanol assists in removing noncovalent interactions thereby increasing the collision cross-section more rapidly over a shorter charge state range in comparison with methanol absent. At the highest charge states observed, methanol causes a greater unfolding than with acid alone therefore providing larger collision cross-sections than for the acid-only samples. This finding illustrates nicely the influence of solvent on observed charge state distributions of protiens.

3.3.4. Elevated pH for tetramer formation

At pH 9.5 five tetramer (Q) species of the form $[Q+nH^+]^{z+}$ for z = 13, 14, 15, 16 and 17 were observable with m/z values of 4959.7, 4605.5, 4298.5, 4030.0 and 3793.0 respectively, although the spectrum was dominated by the z = 17 ion (Fig. 3). The 18^+ species obtained under MS conditions was not observed and three new tetramers (13^+–15^+) were observed perhaps due to desolvation effects. These tetrameric assemblies were successfully transferred to the gas-phase by reducing the pressure in the source region hexapole to 5×10^{-1} mbar and increasing the solution pH to 9.5. Collision cross-sections for the five species were elucidated: (Table 2). The ∼16% increase from 13^+ to 17^+ charge states is relatively small but does indicate a small coulombically driven change in conformation.

3.3.5. Comparison with MOBCAL derived collision cross-sections

Nuclear magnetic resonance (NMR) and X-ray crystallography (XRC) published structures were obtained from the RCSB Protein Data Bank for haemoglobin species. Using the effective hard spheres scattering (EHSS) method within MOBCAL [54,55], theoret-

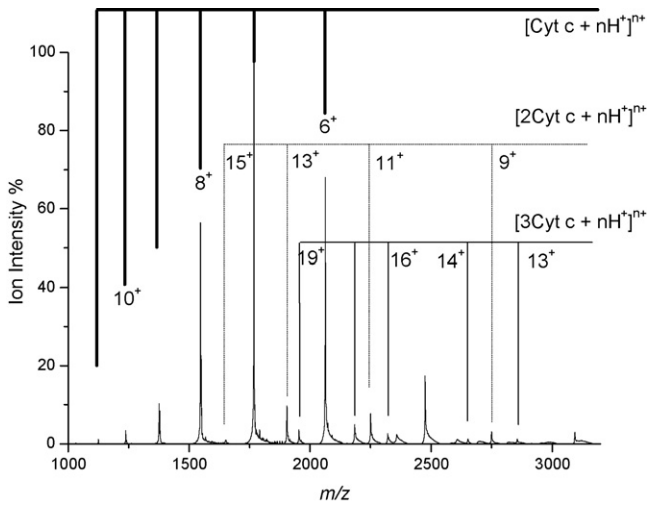

Fig. 4. Cytochrome *c*, 62 μM, sprayed from aqueous solution (pH 5.65) showing monomer, dimer and trimer peaks.

ical cross-sections were produced using the published structures for comparison with the experimental work performed. PDB file 1GZX [56] was used to calculate the collision cross-section for the haemoglobin tetramer (4272 Å^2); 2DN1 [57] was modified to determine the collision cross-sections of both the holoheterodimer, $\alpha^*\beta^*$ (2699 Å^2) and the α_{holo} species (1587 Å^2). By comparing these numbers with experimentally derived values, we note that the dimer and tetramer experimental collision cross-sections are smaller than those calculated theoretically. The tetramer experimental values are smaller by 15–30% compared to the calculated collision cross-section. Holoheterodimer experimental collision cross-sections are ~10–20% smaller than the calculated values. This decrease in collision cross-section is attributed to a contraction of the gas-phase structure in the mass spectrometer. We can speculate that the protein has shrunk on transfer to a solvent (and buffer) free environment.

3.4. IM and IM-MS of cytochrome c multimers

Cytochrome *c* sprayed from aqueous solution (pH 5.65) showed a range of multimeric species (Fig. 4) with the monomer species $[M+nH^+]^{z+}$ for $z = 5–12$ dominating. This is wider than we would expect. The solution is native-like and would be expected to display a narrow distribution of charge indicative of a folded protein, which indeed it does at lower concentrations. Higher charge states may be the result of charge partitioning and dissociation from a higher order multimer such as a dimer.

Dimer ($z = 11^+–19^+$) and trimer ($z = 16^+$, 17^+ and 19^+) signals were observed as favourable pumping and temperature conditions in the source hexapole region allowed aggregates formed in solution to be transferred to the gas-phase. Signals for uneven charged dimers could be assigned only in mass spectrometry experiments as evenly charged dimer m/z values are concomitant with monomers with half the charge i.e., a doubly charged dimer will have the same m/z as a singly charged monomer. Two higher order multimers, 17^+ tetramer (2909 m/z) and 19^+ pentamer (3254 m/z) were repeatedly observed when aqueous samples were sprayed. Ion mobility experiments were performed on aqueous cytochrome *c* samples at 62 μM. Monomer collision cross-sections of cytochrome *c* ranged from 1217 to 2407 Å^2 for 5^+ to 12^+ charge states consistent with the work of Clemmer [29] and as we have previously reported [27] consistent with coulombically driven unfolding.

Dimer (D) cross-sections were obtained for five species: and three trimer (T) collision cross-sections were elucidated (Table 3).

Table 3
Collision cross-sections (Å^2) of aqueous cytochrome *c* (62 μM concentration). Ion mobility data was taken at 300 K temperature, ~3.5 Torr helium, with an elevated source hexapole pressure of ~0.4 mbar for transfer of larger multimeric species.

Charge	Monomer	Dimer	Trimer
5	1217	–	–
6	1243	–	–
7	1546	–	–
8	1865	–	–
9	2066	–	–
10	2228	–	–
11	2255	2586	–
12	2407	–	–
13	–	3248	–
14	–	–	–
15	–	3389	–
16	–	–	3812
17	–	3953	4014
18	–	–	–
19	–	4157	4430

As z increases so does the cross-section for both dimer and trimer. Collision cross-sections of dimer species reveal interesting behaviour which we attribute to a gas-phase unfolding mechanism, the collision cross-sections increase rapidly with z, despite retaining the noncovalent dimeric interaction. Using the PBD file 1CRC [58], two cytochrome *c* monomers have been coarsely docked together to give an approximate dimer arrangement to calculate an EHSS collsion cross-section for this species of 2374 Å^2. This value is smaller than the lowest experimental values obtained for the lowest z, but provides an approximate value for comparison. Dimer unfolding has been shown [59,60] to be accompanied by dissociation to monomers whose charge is dependent upon the initial charge carried by the dimer molecule. Relatively low charged species (e.g., 11^+) dissociate into monomers carrying asymmetrical charge, with one monomer carrying much more of the charge than the other. An intermediate conformation for this would contain one monomer unfolding to a greater extent than the other. As the initial dimer charge increases, this charge asymmetry lessens to a point whereby both monomers dissociate with close to or symmetrical charge as they have unfolded to similar extents and exposed available ionisable sites for protonation. Our measured collision cross-sections for the dimers increase whilst retaining a dimeric interface over a fairly substantial charge state range, significantly greater than that observed with the haemoglobin dimers above or the cytochrome *c* trimers (see below). We only resolve single conformations, suggesting that dimers are stable in this partially unfolded state over the timescale of our experiment.

Protons within the trimer species will be distributed throughout the three subunits. We see a smaller number of trimers and a much smaller change in cross-section with z (Table 3). Unfolding to larger cross-sections will probably not occur until a large number of charges are sequestered on the assembly or, more likely is that dissociation to (i) monomer subunits or (ii) a dimer and a monomer subunit will occur before unfolding. This would explain the small observed population of trimer species and their gas-phase stability will be probed using temperature and collision induced dissociation (CID) in future experiments.

3.5. IM-MS studies of calmodulin

Several groups including us have studied the protein calmodulin with ESI-MS [42,61,62]. Here a range of calcium bound states were observed ranging from apo (0 calcium bound or CaM:0Ca) to 3 calcium bound (CaM:3Ca). Table 4 provides all the measured collision cross-sections. For apo-CaM there are two distinct gas-phase conformations visible at the three lowest charge states ($7^+–9^+$)

Table 4
Collision cross-sections (Å^2) of Calmodulin species containing 0–3 Ca^{2+} bound metal ions. Where two cross-sections are shown for a single charge, these are taken as another conformation of the gas-phase molecule.

Charge	Apo (0 Ca^{2+})	1 Ca^{2+}	2 Ca^{2+}	3 Ca^{2+}
7	1526	1575	1390	1371
	1750	1805	1786	
8	1655	1762	1882	–
	2068	2088		
9	1660	1851	–	–
	2022	2030		
10	1963	1912	–	–
11	2434	2285	–	–
12	2895	2830	–	–
13	2999	2998	–	–
14	3093	3072	–	–
15	3270	3254	–	–
16	3333	–	–	–

which vary by up to 413 Å^2 (8^+). Multiple conformations at low charge states are common to many protein systems and may indicate potential energy minima that the protein is able to access in the gas-phase. Single conformations are observed for all charge states with 10^+ or more charges. Collision cross-sections increase rapidly over a narrow charge state range between $[\text{apo-CaM} + 9H^+]^{9+}$ and $[\text{apo-CaM} + 12H^+]^{12+}$, possibly due to an unfolding event in one of the two protein domains at either termini (N- and C-terminus). A near-linear increase in collision cross-section is observed at higher charge states indicating protein unfolding driven by Coulomb repulsion.

Calcium divalent cations bind at specific binding loops within calmodulin containing acidic residues for electrostatic bonding. Binding is cooperative and addition of a single Ca^{2+} ion allows a second to bind in the same domain. Larger collision cross-sections are observed for all low charge state conformers indicating a local structural rearrangement to incorporate calcium. cross-sections for the higher charged species ($>10^+$) are all smaller than the apo-CaM form and may demonstrate conservation, or tightening of structure due to the calcium-binding event. Due to enhanced electrostatic binding in one region, subsequent protein unfolding takes place to a reduced degree in comparison with the apo form of the protein. This reduced size difference is most pronounced (~6%) for the 11^+ charge state. Comparing the data for the apo and holo forms of CaM it is possible to see that this charge state region is between the folded state (low charge states) and the higher unfolded states ($>12^+$).

MOBCAL calculations on the PDB structure 1CFD [63] (apo-CaM) produced an EHSS collision cross-section of 1870 Å^2. It can be seen that this calculated cross-section is larger than both 7^+ conformers, but lies between both conformers of the 8^+ and 9^+ charge states indicating that the lower charge states produced under these conditions are of comparable size to the NMR structure produced under native-like solution conditions.

Two charge states for CaM:2Ca were observed: 7^+ and 8^+. Two conformers for the 7^+ (1390 Å^2 and 1786 Å^2 respectively) and one conformer for the 8^+ (1882 Å^2) were resolved. The 7^+ conformer of size 1390 Å^2 is significantly smaller than the 7^+ apo conformer (~9%) and is probably due to the C-terminus (where calcium ions have been proposed to bind initially) [64] rearranging to form a more ordered structure due to the enhanced electrostatic interactions. A single measurement for CaM:3Ca was obtained at 1371 Å^2. This is the smallest collision cross-section to have been measured in the experiment for the charge state and is indicative of a well ordered structure upon binding three calcium cations, however it is still larger than we would predict for the fully holo CaM:4Ca species.

4. Consideration of the change in the density of the rotationally averaged cross-section as a protein unfolds in the gas-phase

It is convention in IM-MS studies to describe the 'structure' of analysed components in terms of collision cross-section, converted from the measured mobility according to Eq. (1) above or using a calibration from low field IM-MS data [21]. Whilst this unit of measurement is meaningful to gas-phase researchers, it is somewhat more obtuse to structural biologists. With small biomolecules it is possible to use molecular dynamics simulations to provide an accurate representation of the molecular species observed in an IM-MS experiment and Bowers and Jarrold have led the way in this field of endeavour [65–67] and have provided methods to convert from calculated coordinates to theoretical collision cross-sections [68,69], Countermann and Clemmer have also considered the use of intrinsic size parameters to approximate the structures of amino acids in peptides [70]. With larger systems it is more common to compare the change in collision cross-section from that obtained from a crystal or NMR structure. One of the interesting things about this approach is that invariably the experimental collision cross-section for the lowest recordable charge state is smaller than that obtained from the crystal structure coordinates, as exemplified in the examples given here, and also in the work of Clemmer and co-workers [29,71].

We propose here an alternative representation of conformation recorded in the gas-phase for proteins that are considered to be native or near native. This considers the change in the den-

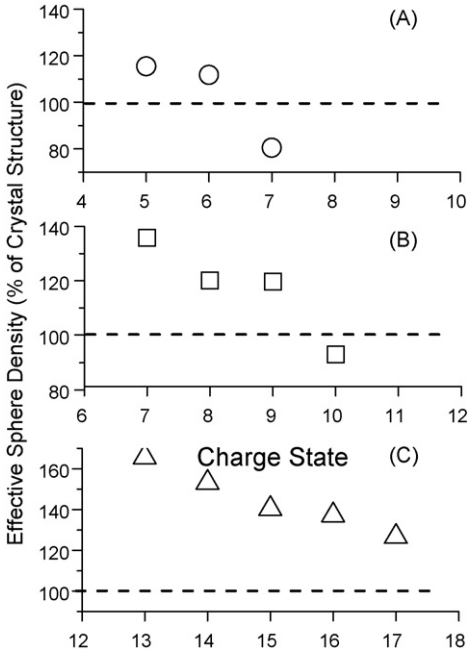

Fig. 5. Plots showing the relationship between the effective sphere density (ESD) measured for the gas-phase molecular ion and charge state for the collision cross-sections that are close to the crystal structure. (A) ESD change as % of crystal structure against low charge state for the experimental data in Table 3 for the cytochrome *c* monomer. The structure 1CRC [59] gives an exact hard spheres calculated cross-section of 1339 Å^2 using the MOBCAL program. This results in a 100% ESD as shown by the line on the plot. (B) ESD change as % of crystal structure against charge state from the experimental data of calmodulin (Table 4) The protein is in its apo form with the smallest conformation only considered for the lower charge states. The structure 1CFD [64] gave an exact hard spheres calculated cross-section of 1870 Å^2 (shown as a line at 100% on the graph). (C) ESD change as a % of crystal structure against charge state for the experimental data in Table 2. The structure 1GZX [56] gave an exact hard sphere cross-section of 4272 Å^2 again shown here as a line at 100% on the graph.

sity of the effective sphere transcribed by the molecular species in the drift cell, essentially its experimental rotationally averaged collision cross-section, compared to the density of the native protein obtained from crystal structure coordinates. For cross-sections obtained from low charge states where the protein is likely to be globular this may provide some insight to a change in protein conformation following desolvation. This relies on an assumption that the protein versus buffer gas occupancy of this sphere is averaged over the experimental timescale, which is safe to make in these low field experiments where the protein will not align in the drift field, and the protein undergoes many rotations on the experimental timescale. Our methodology to convert from measured collision cross-section to decrease in density is simple and contained in supplementary data. Fig. 5 shows the results of this analysis for the proteins cyctochrome *c*, apo-calmodulin and haemoglobin. We have only converted cross-sections that are smaller or a little larger than that found theoretically from the crystal structure co-ordinates. The plots show effective sphere density (ESD) versus charge state and are of course similar to the collision cross-section versus charge state curves, although ESD is proportional to $\Omega^{-3/2}$. Fig. 5 shows clearly that for all proteins the lowest charge states recorded are smaller than the corresponding crystal structure co-ordinates. This effect is most marked for haemoglobin and indicates shrinkage as these molecules are transferred into the solvent free environment of the mass spectrometer, loosing much of the stabilising effects of water and buffer salts that are present in the crystal and therefore perhaps loosing some cavities that would not contain protein but would contribute to its structure.

5. Conclusions

Low field ion mobility mass spectrometry has been successfully implemented to study three metalloprotein systems under a range of solution conditions to determine gas-phase collision cross-sections using the MoQToF. Haemoglobin monomers in both apo and holo forms have been characterised and shown to have a compact structure under physiological pH and extended unfolded structure when the pH is decreased. β_{apo} monomers were observed under both native-like and denaturing conditions providing further evidence for its instability in comparison with its close α-monomer relative. β_{holo} was not observed. Two dimer species, $\alpha^*\beta$ and $\alpha^*\beta^*$ were characterised and shown to be present only under near-native conditions. The $\alpha^*\beta$ semi-haemoglobin intermediate has a similar collision cross-section to that of the holo heterodimer indicating a single loss of the haem group does not alter the structure to a large degree. Under higher pH conditions, a number of tetramer species were observed using mass spectrometry. These all show a lower collision cross-section than that calculated from the crystal structure indicating significant shrinkage in the gas-phase resulting in far denser structures.

Cytochrome *c* monomer, dimer and trimer collision cross-sections were elucidated for a number of charge states. Dimer cross-sections for odd charge states 11^+ to 19^+ have been reported for the first time which allow for significant protein unfolding whilst retaining dimeric interactions. Trimer collision cross-sections have also been reported for the first time.

Calmodulin collision cross-sections were obtained for 0, 1, 2 and 3 calcium bound species with two conformers established for charge states 7^+ to 9^+. Binding of a single calcium ion was shown to increase cross-section at low charge states but decrease cross-section at higher charge states ($\geq 11^+$). This is attributed to structural and noncovalent interaction rearrangements occurring within the molecule. Upon binding a second calcium ion, a tightening of the structure was observed with a decrease in cross-section of the 7^+ charge state perhaps indicating domain folding at the C-terminus. Finally, a single 3 bound calcium CaM complex cross-section was determined. This was the smallest of all collision cross-sections elucidated showing the trend towards to a more compact structure with further calcium cations added.

Acknowledgments

This research was supported by the EPSRC grants GR/S77639/01 and EP/C541561/1 and in particular *via* the award of an Advanced Research Fellowship to PEB and studentships to BJM and (in conjunction with the RSC Analytical Trust Fund) to PAF. We also had support from the Royal Society, the British Mass Spectrometry Society, and Waters MS Technologies Centre, and in particular we thank Steven Pringle, Kevin Giles, Jason Wildgoose and Robert Bateman. We also are grateful for the continuing support from the School of Chemistry at the University of Edinburgh.

Appendix A. Supplementary data

Supplementary data associated with this article can be found, in the online version, at doi:10.1016/j.ijms.2009.02.024.

References

[1] P.E. Barran, N.C. Polfer, D.J. Campopiano, D.J. Clarke, P.R.R. Langridge-Smith, R.J. Langley, J.R.W. Govan, A. Maxwell, J.R. Dorin, R.P. Millar, M.T. Bowers, Int. J. Mass Spectrom. 240 (2005) 273.
[2] T. Wyttenbach, G. von Helden, M.T. Bowers, J. Am. Chem. Soc. 118 (35) (1996) 8355.
[3] D.E. Clemmer, M.F. Jarrold, J. Mass Spectrom. 32 (6) (1997) 577.
[4] J.B. Fenn, M. Mann, C.K. Meng, S.F. Wong, C.M. Whitehouse, Science 246 (1989) 64.
[5] N.B. Cech, C.G. Enke, Mass Spectrom. Rev. 20 (6) (2001) 362.
[6] M. Wilm, M. Mann, Anal. Chem. 68 (1) (1996) 1.
[7] D. Liu, T. Wyttenbach, P.E. Barran, M.T. Bowers, J. Am. Chem. Soc. 125 (28) (2003) 8458.
[8] F. Sobott, C. Robinson, Int. J. Mass Spectrom. 236 (1–3) (2004) 25.
[9] A.A. Rostom, C.V. Robinson, J. Am. Chem. Soc. 121 (19) (1999) 4718.
[10] J.L.P. Benesch, B.T. Ruotolo, D.A. Simmons, C.V. Robinson, Chem. Rev. 107 (8) (2007) 3544.
[11] A.J.R. Heck, R.H.H. van den Heuvel, Mass Spectrom. Rev. 23 (5) (2004) 368.
[12] R.H.H. van den Heuvel, E. vanDuijn, H. Mazon, S.A. Synowsky, K. Lorenzen, C. Versluis, S.J.J. Brouns, D. Langridge, J. vanderOost, J. Hoyes, A.J.R. Heck, Anal. Chem. 78 (21) (2006) 7473.
[13] J.L.P. Benesch, C.V. Robinson, Curr. Opin. Struct. Biol. 16 (2) (2006) 245.
[14] M.J. Cohen, F.W. Karasek, J. Chromatogr. Sci. 8 (6) (1970) 330.
[15] C. Wu, W.F. Siems, J. Klasmeier, H.H. Hill Jr., Anal. Chem. 72 (2) (2000) 391.
[16] R. Fromherz, G. Gantefor, A.A. Shvartsburg, Phys. Rev. Lett. 89 (8) (2002) 083001.
[17] R. Guevremont, Can. J. Anal. Sci. Spectrosc. 49 (3) (2004) 105.
[18] A.A. Shvartsburg, F. Li, K. Tang, R.D. Smith, Anal. Chem. 78 (10) (2006) 3304.
[19] K. Giles, S.D. Pringle, K.R. Worthington, D. Little, J.L. Wildgoose, R.H. Bateman, Rapid Commun. Mass Spectrom. 18 (20) (2004) 2401.
[20] S.D. Pringle, K. Giles, J.L. Wildgoose, J.P. Williams, S.E. Slade, K. Thalassinos, R.H. Bateman, M.T. Bowers, J.H. Scrivens, Int. J. Mass Spectrom. 261 (1) (2007) 1.
[21] B.T. Ruotolo, J.L. Benesch, A.M. Sandercock, S.J. Hyung, C.V. Robinson, Nat. Protoc. 3 (7) (2008) 1139.
[22] A.J.H. Borysik, P. Read, D.R. Little, R.H. Bateman, S.E. Radford, A.E. Ashcroft, Rapid Commun. Mass Spectrom. 18 (19) (2004) 2229.
[23] T. Wyttenbach, P.R. Kemper, M.T. Bowers, Int. J. Mass Spectrom. 212 (1–3) (2001) 13.
[24] Y. Mao, J. Woenckhaus, J. Kolafa, M.A. Ratner, M.F. Jarrold, J. Am. Chem. Soc. 121 (12) (1999) 2712.
[25] S.L. Koeniger, S.I. Merenbloom, S.J. Valentine, M.F. Jarrold, H.R. Udseth, R.D. Smith, D.E. Clemmer, Anal. Chem. 78 (12) (2006) 4161.
[26] A.B. Kanu, P. Dwivedi, M. Tam, L. Matz, H.H. Hill, J. Mass Spectrom. 43 (1) (2008) 1.
[27] B.J. McCullough, J. Kalapothakis, H. Eastwood, P. Kemper, D. MacMillan, K. Taylor, J. Dorin, P.E. Barran, Anal. Chem. 80 (16) (2008) 6336.
[28] E.A. Mason, E.W. McDaniel, Transport Properties of Ions in Gases, Wiley, New York, 1988.
[29] D.E. Clemmer, R.R. Hudgins, M.F. Jarrold, J. Am. Chem. Soc. 117 (40) (1995) 10141.
[30] M.F. Jarrold, Acc. Chem. Res. 32 (4) (1999) 360.
[31] E.R. Badman, S. Myung, D.E. Clemmer, J. Am. Soc. Mass Spectrom. 16 (9) (2005) 1493.
[32] J.D. Henion, Y.-T.Y.-L.H. Li, Am. Soc. Mass Spectrom. 4 (1993) 631.
[33] W.P. Griffith, I.A. Kaltashov, Curr. Org. Chem. 10 (5) (2006) 535.
[34] A. Schmidt, M. Karas, J. Am. Soc. Mass Spectrom. 12 (10) (2001) 1092.
[35] D.S. Gross, Y. Zhao, E.R. Williams, J. Am. Soc. Mass Spectrom. 8 (5) (1997) 519.
[36] G. Vasudevan, M.J. McDonald, J. Biol. Chem. 272 (1) (1997) 517.
[37] G. Vasudevan, M.J. McDonald, Curr. Protein Pept. Sci. 3 (4) (2002) 461.

[38] W.P. Griffith, I.A. Kaltashov, Biochemistry 42 (33) (2003) 10024.
[39] B.L. Boys, M.C. Kuprowski, L. Konermann, Biochemistry 46 (37) (2007) 10675.
[40] W.P. Griffith, I.A. Kaltashov, Biochemistry 46 (7) (2007) 2020.
[41] W.E. Meador, A.R. Means, F.A. Quiocho, Science 262 (5140) (1993) 1718.
[42] S. Shirran, P. Garnaud, S. Daff, D. McMillan, P. Barran, J. Royal Soc. Interf. 2 (5) (2005) 465.
[43] H. Kuboniwa, N. Tjandra, S. Grzesiek, H. Ren, C.B. Klee, A. Bax, Nature Struct. Biol. 2 (1995) 768.
[44] A. Persechini, R.H. Kretsinger, J. Biol. Chem. 263 (25) (1988) 12175.
[45] C. Versluis, A.J.R. Heck, Int. J. Mass Spectrom. 210 (1–3) (2001) 637.
[46] J.F. de la Mora, Anal. Chim. Acta 406 (1) (2000) 93.
[47] J. Karen, B.L.S. Light-Wahl, Richard D. Smith, J. Am. Chem. Soc. 116 (1994) 5271.
[48] L. Konermann, D.A. Simmons, Mass Spectrom. Rev. 22 (1) (2003) 1.
[49] Y. Bai, T.R. Sosnick, L. Mayne, S.W. Englander, Science 269 (1995) 192.
[50] S.K. Chowdhury, V. Katta, B.T. Chait, J. Am. Chem. Soc. 112 (24) (1990) 9012.
[51] J.A. Loo, R.R.O. Loo, H.R. Udseth, C.G. Edmonds, R.D. Smith, Rapid Commun. Mass Spectrom. 5 (3) (1991) 101.
[52] K.R. Babu, D.J. Douglas, Biochemistry 39 (47) (2000) 14702.
[53] A.A. Komar, A. Kommer, I.A. Krasheninnikov, A.S. Spirin, J. Biol. Chem. 272 (16) (1997) 10646.
[54] A.A. Shvartsburg, M.F. Jarrold, Chem. Phys. Lett. 261 (1–2) (1996) 86.
[55] M.F. Mesleh, J.M. Hunter, A.A. Shvartsburg, G.C. Schatz, M.F. Jarrold, J. Phys. Chem. 100 (40) (1996) 16082.
[56] M. Paoli, R. Liddington, J. Tame, A. Wilkinson, G. Dodson, J. Mol. Biol. 256 (4) (1996) 775.
[57] S.-Y. Park, T. Yokoyama, N. Shibayama, Y. Shiro, J.R.H. Tame, J. Mol. Biol. 360 (3) (2006) 690.
[58] R. Sanishvili, K.W. Volz, E.M. Westbrook, E. Margoliash, Structure 3 (7) (1995) 707.
[59] J.C. Jurchen, E.R. Williams, J. Am. Chem. Soc. 125 (9) (2003) 2817.
[60] J.C. Jurchen, D.E. Garcia, E.R. Williams, J. Am. Soc. Mass Spectrom. 15 (10) (2004) 1408.
[61] M.M. Zhu, D.L. Rempel, J. Zhao, D.E. Giblin, M.L. Gross, Biochemistry 42 (51) (2003) 15388.
[62] M. Nousiainen, P.J. Derrick, D. Lafitte, P. Vainiotalo, Biophys. J. 85 (1) (2003) 491.
[63] H. Kuboniwa, N. Tjandra, S. Grzesiek, H. Ren, C.B. Klee, A. Bax, Nat. Struct. Mol. Biol. 2 (9) (1995) 768.
[64] D. Lafitte, J.P. Capony, G. Grassy, J. Haiech, B. Calas, Biochemistry 34 (42) (1995) 13825.
[65] A. Baumketner, S.L. Bernstein, T. Wyttenbach, G. Bitan, D.B. Teplow, M.T. Bowers, J.E. Shea, Protein Sci. 15 (3) (2006) 420.
[66] Y. Mao, M.A. Ratner, M.F. Jarrold, J. Phys. Chem. B 103 (45) (1999) 10017.
[67] T. Wyttenbach, J.E. Bushnell, M.T. Bowers, J. Am. Chem. Soc. 120 (20) (1998) 5098.
[68] T. Wyttenbach, G. von Helden, J.J. Batka Jr., D. Carlat, M.T. Bowers, J. Am. Soc. Mass Spectrom. 8 (3) (1997) 275.
[69] A.A. Shvartsburg, G.C. Schatz, M.F. Jarrold, J. Chem. Phys. 108 (6) (1998) 2416.
[70] A.E. Counterman, D.E. Clemmer, J. Am. Chem. Soc. 121 (16) (1999) 4031.
[71] S. Myung, E.R. Badman, Y.J. Lee, D.E. Clemmer, J. Phys. Chem. A 106 (42) (2002) 9976.